JOURNAL OF Materials CHEMISTRY

Blue luminescence in yttrium and gadolinium niobates caused by bismuth. The importance of non-bonding ns^2 valence orbital electrons

Xiping Jing,[a] Carol Gibbons,[a] David Nicholas,[a] Jack Silver,*[a] Aron Vecht[a] and Christopher S. Frampton[b]

[a]*Centre for Phosphors and Display Materials, University of Greenwich, Wellington Street, London, UK SE18 6PF*
[b]*Roche Discovery, Welwyn, PO Box 8, Welwyn Garden City, Herts, UK A17 2AY*

Received 15th July 1999, Accepted 14th September 1999

A blue luminescent emission band (440 nm) has been optimised in $Y_{1-x}Bi_xNbO$ ($x=0.005$) for low voltage phosphor applications. The material has useful properties when compared to a commercially available phosphor. The role of the Bi^{3+} ion dopant is discussed in this lattice and in the related $Gd_{1-x}Bi_xNbO_4$ lattice. The movement of the emission band with $\%Bi^{3+}$ is rationalised using a simple electronic band structure model. It is demonstrated that the nature (symmetry) of the chemical environment of the Bi^{3+} is important for the influence of the cation on the luminescent properties.

This work is part of our program to produce phosphors for low voltage applications. Although adequate green and red phosphors are currently available, no suitable, non-sulfide stable blue phosphor has been developed. One reason for this is because zinc sulfide (silver doped), which is probably one of the most efficient phosphors known, could meet cathode ray requirements, and this resulted in other blue emitting phosphors being neglected. In stark contrast, tremendous effort was devoted to the production of red phosphors for coloured television, which resulted in a range of red systems based on europium doped yttrium oxide, yttrium orthovanadate or yttrium oxysulfide.

The luminescence of ns^2 ions like $Sb^{3+}(5s^2)$, Bi^{3+} and $Pb^{2+}(6s^2)$ has, over the last decade, received considerable attention.[1–9] Studies on mixed oxide materials containing transition-metal ions with noble-gas configurations have been reported,[1–5] and two extreme situations have been shown to occur. Firstly, the excited state can be localised on the octahedra. Here, the emission consists of a Stokes shifted broad band, and the quenching temperature depends on the amount of relaxation.[1,2] In the second case, the excited state is delocalised over the octahedra (into the lattice). The amount of such delocalisation is said to be dependent on the angle between the corner sharing octahedra.[6–8] In practice, if the metal–oxygen–metal angle approaches 180°, the orbital overlap increases. Blasse and coworkers[9] have recently shown that ns^2 ions in symmetrical coordination sites influence the luminescence properties of transition metal oxy-complexes. However, if the ns^2 ions are asymmetrically coordinated, their influence is limited.

The ns^2 ions have previously been shown to have interesting properties. We have described the effects of high symmetry environments in compounds of elements with non-bonding valence-shell ns^2 outer electron configurations[10] and come to similar conclusions to Blasse and coworkers.[9] The stereochemistry of most p-block elements in lower oxidation states is dominated by the presence of filled non-bonding lone-pair orbitals. Indeed, the environments of these elements in many compounds of Sn(II), Pb(II), As(III), Sb(III), Bi(III), Se(IV), Te(IV) and Po(IV) are found to be distorted by the presence of these lone-pair orbitals. However, there are a number of compounds in which these elements are found in regular octahedral sites.[11–15] Previous to our work,[10] these regular environments had been explained either in terms of the accommodation of the ns^2 electrons in a_{1g} antibonding orbitals[13] or in terms of the absence of distorting crystal field effects.[16] We pointed out that all of the solid compounds containing significant amounts of ns^2 elements in high-symmetry sites are coloured and that many manifest metallic or semi-conducting electrical properties.[10]

The conclusion of much of our work[10,17,18] on the properties and stereochemistries of p-block elements in lower oxidation states suggest that high symmetry solid-state environments for most of these elements are only found for compounds in which the distorting effect of the non-bonding lone-pair electrons is reduced by the availability of a low-lying, empty delocalised band (low energy) in the structure, into which these electrons can be partially transferred. By taking into account exact details of the orbital electronegativities of the elements involved in bonding in any given compounds, this model was able to explain the colours and properties of compounds with high symmetry ns^2-element environments better than any previous model. The model was extended to explain colour in tetragonal SnO and other materials which have relatively short metal–metal contacts because, in such cases, the ns^2 element is not only supplying the donor electrons but also forming the band by mutual overlap of its empty d-orbitals.[10]

Essential evidence indicated:

1 the highly symmetric nature of the Sn(II) electronic environment in compounds such as C_5SnBr_3 (as shown by Mössbauer spectra).[10–12,17,19–21] These showed the presence of single absorption lines that arise only from highly symmetric electronic environments where there is no 5s–5p mixing.

2 That some of the $5s^2$ electron density was transferred from the Sn(II) into low energy delocalised bands in the structure (again from the Mössbauer spectra). The chemical isomer shifts of the single absorption lines were not as high as expected (indicating less 's' electron density at the nucleus than expected) and thus it could be inferred that the '5s' electron density was transferring elsewhere in the structures.

It may be thought that the crystal structures of the ns^2 compounds depend on an interplay between lowering the electronic energy of the ns^2 ion by distortion of the coordination environment from a centrosymmetric arrangement when *n*s–*n*p mixing is not possible to a lower symmetry

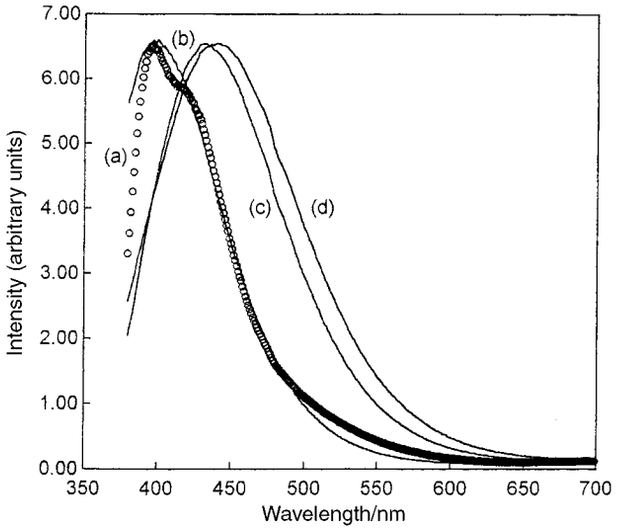

Fig. 1 CL spectra of (a) P47, (b) $YNbO_4$, (c) $GdNbO_4$:Bi and (d) $YNbO_4$:Bi; electron beam: 2000 V, 17 μA and 1.0 cm diameter.

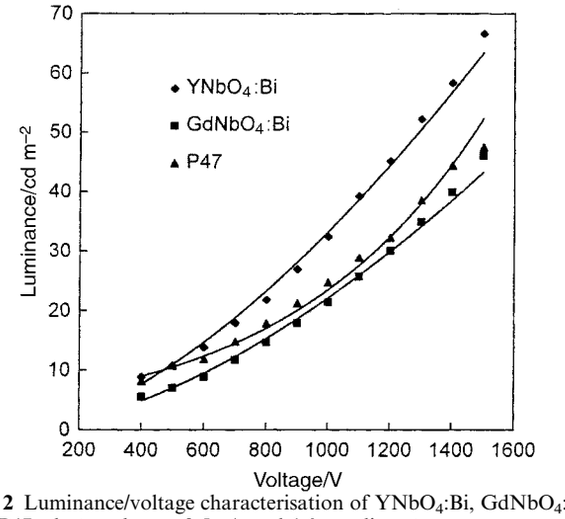

Fig. 2 Luminance/voltage characterisation of $YNbO_4$:Bi, $GdNbO_4$:Bi and P47; electron beam: 8.5 μA and 1.0 cm diameter.

where such mixing is possible; and raising of the Madelung energy by the distortion. Following from this, whether or not the structure would distort depends on the competition between the two effects. For a small distortion, both would vary with the square of the displacement along a distortion coordinate. However, in practice, distorted low valence p-block element-electronic environments are only found in compounds where the nearest ligands are first row elements that contain no empty low-lying 'd' orbitals. In such compounds, the *n*s–*n*p mixing of the two non-bonding electrons results in the presence of a stereochemically active lone-pair which distorts the structure. For Sn(II) compounds, such distorted electronic environments give rise to an electric field gradient across the tin nucleus, which is manifested in the Mössbauer spectrum by the presence of a quadrupole splitting (seen as two absorption lines). It can therefore be argued that there are, in fact, two ways of lowering the electronic energy of an ns^2 ion. One is by distortion of the coordination environment by *n*s–*n*p mixing, and the other is by transfer of some of the 's' electron density into a low-lying delocalised band.

Several of our studies examined small amounts of ns^2 dopant ion on colourless or pale coloured lattices,[12,18–22] at very low concentrations (<0.5% of ns^2 active element dopant), little change of colour was observed.[12,22] However it could be inferred that the ns^2 electrons were at the top of the valence band.[22] Such a picture is similar to that of Blasse and coworkers[9] and will be discussed further in the present work to investigate the influence of an ns^2 cation, in this case Bi^{3+}, on the luminescence properties of the rare-earth element–transition-metal element oxides $YNbO_4$ and $GdNbO_4$.

The rare-earth element niobates $LnNbO_4$ (Ln = Y, La, Gd, Lu) have been shown to exhibit deep-blue emission with a high quenching temperature,[23–25] so that some luminescence is still visible at room temperature.

The current investigation has concentrated on these highly refractory oxides as they were likely to be stable, and utilizes Bi^{3+} as the activator to see if narrow band, efficient blue filter-free systems could be developed. We have concentrated on $YNbO_4$ oxides. These materials have previously been the subject of two patents.[26,27] The first also mentions $GdNbO_4$ and claims luminescent properties when excited by ultraviolet radiation.[26] The second patent claims specific dopant levels of bismuth in the $Gd_{1-x}Bi_xNbO_4$ lattice, and specifies that resultant materials emit light in the blue region of the spectrum when excited with ultraviolet light or cathode rays.[27] The optimum dopant levels claimed are $0<x<0.2$.[27] This work is more fully discussed later; the phosphors were not studied for their low voltage cathode ray phosphor characteristics, but were developed for fluorescent lighting.

We report here, low voltage luminescence studies on $Y_{1-x}Bi_xNbO_4$ and $Gd_{1-x}Bi_xNbO_4$ phosphors. Preliminary details of part of this work have been presented elsewhere.[28]

Experimental

Samples were prepared through solid-state reactions at high temperatures. Y_2O_3, Gd_2O_3, Nb_2O_5 and Bi_2O_3 were used as starting materials (purity >99.99%). The starting materials were weighed out accurately in the required amounts and were mixed together using an agate mortar and pestle. During grinding, a small amount of acetone was added in order to mix the materials homogeneously. The samples were first fired in Al_2O_3 crucibles at 1250 °C for 2 h. The second firing was carried out at 1400 °C for 30 min. Between the firing, the samples were reground. All samples were reproduced at least three times. XRF analyses from Ceram Research and in-house analyses on several samples, gave bismuth contents very close to expected values.

The phase present in the samples was determined using an X-ray diffractometer (Siemens D5000). XRD patterns of all the samples are in accord with JCPDS files 23-1486 for $YNbO_4$ and 22-1104 for $GdNbO_4$, respectively. The morphology of selected samples was observed by using SEM (Cambridge Instruments, Stereoscan 90).

For cathodoluminescence (CL) measurement, the phosphor samples were coated on aluminium stubs using electrophoresis. Propan-2-ol containing 5×10^{-4} M $Mg(NO_3)_2$ was used as an electrolyte solution. Phosphor suspensions were made by dispersing a small amount of phosphor (*ca.* 0.5 g) into the electrolyte solution (50 ml). In order to obtain better dispersion, the suspensions were vibrated in an ultrasonic bath for several minutes. The electrophoresis voltage used was 200 V and the coating time was varied from 2 to 10 min, depending on the sample. The coating thickness was *ca.* 5 mg cm^{-2}. The coated Al stubs were then placed into a chamber, which was evacuated to a pressure of *ca.* 10^{-6} Torr. A Kimbal physics Inc. (Walton. NH) model EGPS-7 electron gun was employed to excite the samples. The dc measurements were undertaken with an electron beam size of 1.0 cm diameter. A PhotoResearch Pritchard PR880 photometer was used to measure luminance and a Bentham monochromator/detector system was used to record CL spectra. The host lattices $YNbO_4$ and $GdNbO_4$ manifested very poor luminescence without the presence of the Bi^{3+} activator.

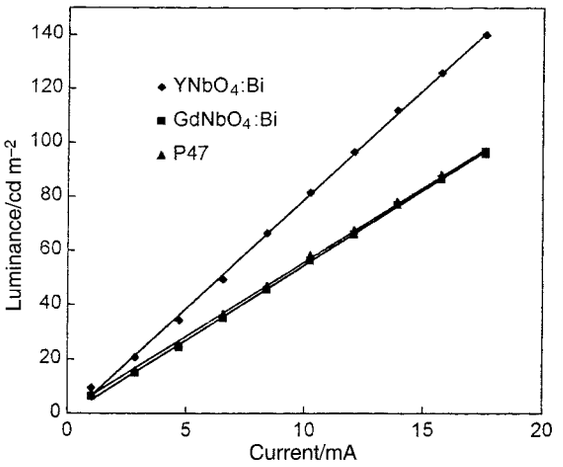

Fig. 3 Luminance/voltage characterisation of $YNbO_4$:Bi, $GdNbO_4$:Bi and P47; electron beam: 1500 V and 1.0 cm diameter.

Results and discussion

The spectra under CL excitation of both $Y_{1-x}Bi_xNbO_4$ and $Gd_{1-x}Bi_xNbO_4$ ($x=0.005$ in both compounds) are compared with that of P47 Y_2SiO_5:Ce obtained from Nichia and $YNbO_4$ in Fig. 1. Both of the spectra are slightly broader towards both the short and longer wavelengths.

In comparison to the commercially available P47, $YNbO_4$ doped with Bi^{3+} ($x=0.005$) showed higher luminance and efficiency (see Figs. 1–3). In addition, this phosphor was better than its Gd analogue under CL excitation, unlike the results under photoluminescence reported by others.[29]

Considerable further synthetic studies were undertaken to ascertain the optimum composition of the parent lattice which was found for a 1:1 Y to Nb ratio.[28]

Although in our preliminary investigation we found it was necessary to have excess Nb_2O_5 present to achieve a 1:1 compound, our present heating and firing regime did not require excess Nb_2O_5.

Fig. 4 shows the cathodoluminance dependence of $Y_{1-x}Bi_xNbO_4$ with Bi content x. The optimum Bi level was found to be 0.005, the same final result was found for Bi in the $Gd_{1-x}Bi_xNbO_4$ system.

From our current samples, which for the Y compound has particle sizes in the range 1–5 μm (Fig. 5), and for the Gd compound 2–7 μm (Fig. 6), we have recorded efficiencies of *ca.*

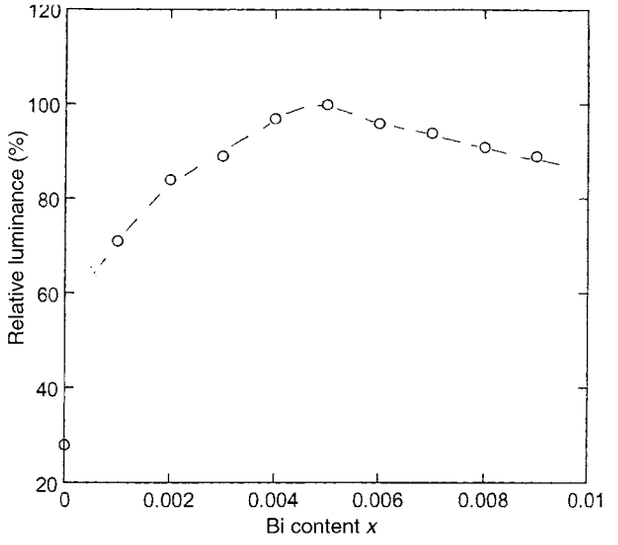

Fig. 4 Variation of CL luminance of $Y_{1-x}Bi_xNbO_4$ with Bi content (x); electron beam: 1500 V, 8.5 μA and 1.0 cm diameter.

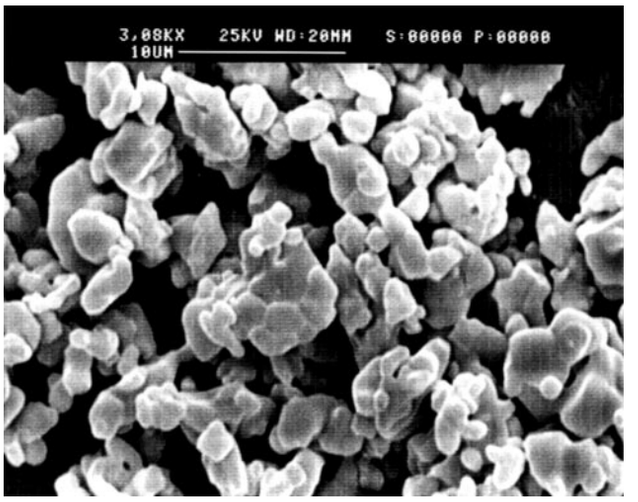

Fig. 5 SEM photograph of $YNbO_4$:Bi particles.

1.3 lm W^{-1} (for $YNbO_4$:Bi) and 0.89 lm W^{-1} (for $GdNbO_4$:Bi) compared to 0.91 L W^{-1} for P47 measured under identical conditions.

Effect of crystal structure

The Fergusonite structure of $YNbO_4$ is considered as a distorted scheelite structure. In the scheelite, $CaWO_4$, structure, the tungsten is surrounded by four oxygen ions. These tetrahedra can be considered as isolated molecular groups.[25] In monoclinic fergusonite, $YNbO_4$, this view is not valid as two of the four next-nearest oxygen atoms are at a closer distance and the other two a longer distance than in the scheelite structure.[30] The coordination around the Nb can be considered as 4+2 with the four Nb–O bond lengths in the range 1.84–1.95 Å, and the other two at 2.44 Å.[25,30] From this, the monoclinic fergusonite structure is in between the scheelite structure with isolated groups and crystal structures of niobates with octahedral niobate groups.[30]

Indeed, decay measurements on the blue emission, which is the intrinsic niobate luminescence, provide evidence that the luminescence cannot be understood on the basis of a tetrahedral niobate group.[25]

Luminescence studies of both α- and β-$BiNbO_4$ phases have been reported, these materials do not luminesce at room temperature but show broad band emission at low temperatures, *i.e.* 4.2 K.[1] The β-phase has an emission band further towards the blue (485 nm) and the coordination of the Bi^{3+} is more symmetrical than in the α-phase.[1,9,31–33] Fig. 7 shows the maximum emission peak variation for $Y_{1-x}Bi_xNbO_4$ as a

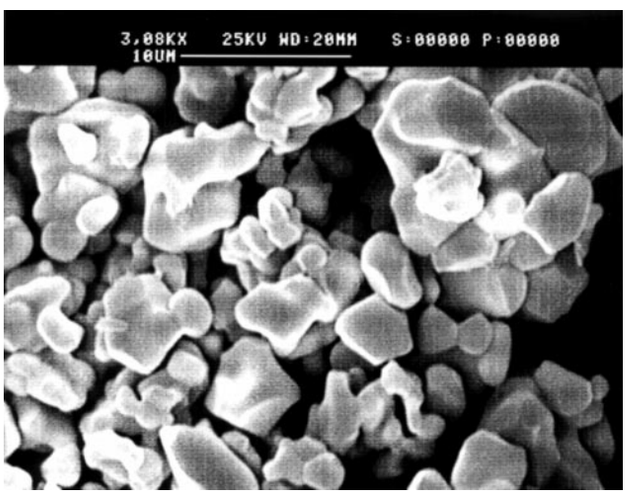

Fig. 6 SEM photograph of $GdNbO_4$:Bi particles.

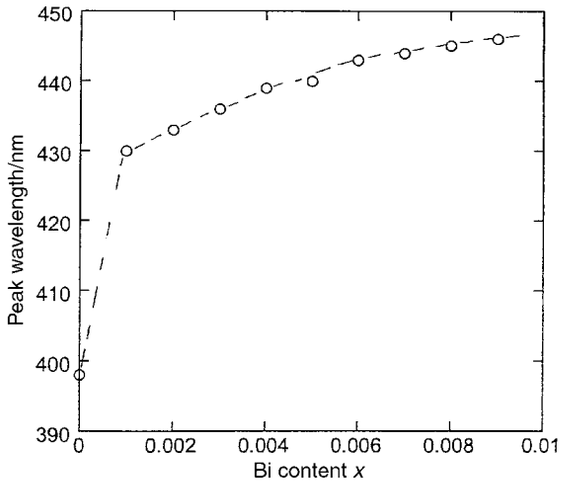

Fig. 7 Peak wavelength variation of $Y_{1-x}Bi_xNbO_4$ spectra with Bi content (x); electron beam: 1500 V, 8.5 μA and 1.0 cm diameter.

function of Bi content at 298 K. A similar variation was observed for $Gd_{1-x}Bi_xNbO_4$ (starting at $\lambda_{max}=485$ nm).

The question that must now be asked is: what is the nature of the $6s^2$ electronic states in these compounds? and what is the energy of the $6s^2$ state? Obviously, the energy of the $6s^2$ state will be lowered by 6s–6p mixing in distorted environments, and if the $6s^2$ cation is in a regular centrosymmetric environment it would probably lie at the top or just above the valence band in the bandgap. For a band model, we turn to recent work by Blasse and coworkers[9] who proposed a model to explain the electronic band structure for β-Bi(Nb/Ta)O_4 justified from known crystal structural data. The reasonable assumption is made that the $6s^2$ valence band levels lie just above the $2p(O^{2-})$ valence band levels. Absorption transitions are determined by the $6s^2$–4d/5d transition, which takes place at lower energy than the 2p–4d/5d charge-transfer transition.[9] Such an energy band model has been calculated for $PbTiO_3$ in which the Pb^{2+} ion has a $6s^2$ band.[34]

The initial peak maximum of 398 nm (Fig. 7) is for the undoped $YNbO_4$ lattice and we note that other workers[25] reported this band at 405 nm. On adding Bi_x ($x=0.001$) the emission peak moves abruptly to 430 nm and then gradually increases towards 450 nm as x increases towards 0.01. As we found no evidence of a change in lattice size for these levels of dopant, we conclude that the lattice remains relatively unchanged. This means that the energy gap (E_g) between the valence band and the conduction band would be expected to remain the same if Bi^{3+} was not affecting the valence band. The schematic model of the electronic band structure we propose is similar to that of Blasse and coworkers[3,9] (Fig. 8), except that we suggest the Y 4d orbitals will also contribute to the conduction band. The conduction band is assumed to be

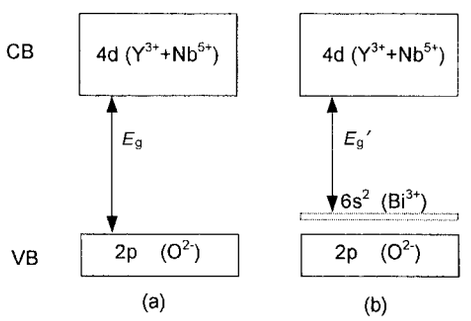

Fig. 8 Schematic model of the electronic band structure of (a) $YNbO_4$ and (b) $Y_{1-x}Bi_xNbO_4$ ($0<x<0.1$). Only the band gap and Bi^{3+} band are nearly to scale relative to one another; the rest of valence and conduction bands are not to scale.

made up also of the Nb^{5+}4d orbitals, and the valence band (before Bi doping) is made up from O^{2-} 2p populated orbitals. When Bi^{3+} ions are added to this model, their $6s^2$ valence electrons lie on top of the O^{2-} 2p valence band levels. The presence of the Bi^{3+} $6s^2$ electron levels causes the energy gap to decrease to E_g', and this decrease will be proportional to the amount of Bi^{3+} present. This is seen in the change of wavelength of the emission peak with Bi^{3+} content (Fig. 7). The change in wavelength would be expected to continue until a Bi^{3+} content was introduced that would cause lattice distortion and disturb either the energy of the conduction band orbitals or both the valence and conduction band orbitals. At $x=0.1$, the emission peak is around 460 nm, and although in this compound the lattice is not distorted an increase in lattice size is observed so that the relative positions of the conduction and valence bands may alter a little and hence, as x increases above 0.01, less effect on the wavelength is observed. Evidence for E_g' being smaller than E_g is also found in the diffuse reflectance spectra of $YNbO_4$ and $YNbO_4$:Bi (shown in Fig. 3 of ref. 29). The width of the former is larger than the latter and begins at higher energy (>240 nm) *cf.* 305 nm for the latter.

The abrupt change in the wavelength of the emission band from 398 to 430 nm on the initial addition of Bi_x ($x=0.001$) is noteworthy. The obvious interpretation is that initially, the dopant Bi^{3+} forms localized levels above the top of the $2p(O^{2-})$ valence band. These levels must be separated by the order of a few kT above the valence band or their ns^2 electrons would not be able to initially fill holes in the valence band that occur when electrons from this band are raised to the conduction band during cathode ray bombardment. The resulting holes on the localized levels then account for the luminescence by radiative transitions of the free electrons in the conduction band to these levels. As more Bi^{3+} ions are added to the $YNbO_4$ lattice, more levels are introduced forming a continuous band made up of non-bonding valence orbital $6s^2(Bi^{3+})$ electrons. The major part is that the initial abrupt change in wavelength indicates that this band is separated slightly from the top of the valence band by the order of a few kT. The initial emission peak shift is *ca.* 8%, thus, the $6s^2$ band electron must begin about one twelfth of the E_g above the top of the $2p(O^{2-})$ valence band. The $6s^2$ band width increases (as more Bi^{3+} is introduced) to about one twentieth (*i.e.* emission band shift from 430 to 450 nm, Fig. 7) of the band gap by around $x=0.01$. In $YNbO_4$ the Y^{3+} coordination is more symmetrical than that of Bi^{3+} in β-$BiNbO_4$.[30,35] Hence, when Bi^{3+} replaces Y in the $Y_{1-x}Bi_xNbO_4$ lattice ($x<0.01$), it will be on the Y positions and in a more symmetrical environment than it has in α- or β-$BiNbO_4$.

It is worth considering whether the sudden change in the emission band wavelength is an example of a Mott transition.[36] In such a transition, there is a change from non-metallic to metallic conduction when the concentration of impurity centres exceeds a certain critical value, n_c, with consequential changes in other physical properties. Mott[36] demonstrated that this critical concentration was related to the radius of the far Bohr orbit of the impurity atom (a_H) by an expression of the form

$$n_c^{1/3} a_H = K$$

Edwards and Sienko[37] redefined a_H as a realistic radius of the wavefunction and, having reviewed a wide range of experimental data, estimated K as 0.26 ± 0.05.

The initial Bi^{3+} concentration (x) of 0.001 puts an upper limit of n_c as 1.16×10^{19} cm^{-3}, which implies a lower limit of a_H at 11.5 ± 2 Å. As the radius a_H varies as the cube root of the concentration, it is remarkably insensitive to n_c. If the critical concentration was as low as 0.0001, then the radius would be 25 ± 4 Å.

An estimate of a_H can also be made from the relation[37]

$$a_H = K\hbar^2/M_{eff}e^2$$

Here, K is the static dielectric constant (relative permittivity) and M_{eff} is the effective electron mass. Redefining M_{eff} as rm, m being the normal electron mass gives

$$a_H = 0.53(K/r)\text{Å}$$

A reasonable value of K for an ionic oxide might be 5, while r for a semiconductor would be of the order of 0.1,[38] putting a_H at about 25 Å, a figure typical of those quoted in the literature for impurity atoms in semiconductors,[37] and certainly consistent with a value of x in the range 0.0001–0.001.

These calculations justify an electronic band structure model for the $Y_{1-x}Bi_xNbO_4$ phosphor materials with x values in the range 0.001–0.01. However, it must be asked if a band model is necessary and, moreover, at the insulator–metal transition (Mott transition) a high-density electron–hole plasma state would be expected. This would emit light with a broad-band spectrum. Now, although the emission band is not narrow (Fig. 1), if it is assumed to be symmetrical, then the width is of the order of 200 nm. The question is, can it be described as broad band? So, although the calculations fit a Mott transition, the band width perhaps does not justify the approach.

The alternative explanation is to think only in terms of a localised state model. Such a model could explain the change in wavelength with dopant level by assuming the dielectric constant of the solid changes with increased doping.

It is useful at this point to consider Tl^+ ions doped into alkali metal halide crystals such as NaCl or KI. Such a model as that of the original work of Seitz[39] is worth noting. The $6s^2$ ground state is expressed by $^1S_0$. The 6s–6p first excited state is a triplet $^3P_1$ and a singlet $^1P_1$. The order of these states in increasing energy is $^3P_0$, $^3P_1$, $^3P_2$ and $^1P_1$. When the Tl^+ is in an alkali metal halide host, and if it occupies a cation site, it is in an octahedral crystal field. The energy levels of the Tl^+ ions are labelled using the irreducible representation of the O_h point group. The labelling is as follows: For the ground state, $^1S_0 \rightarrow {}^1A_{1g}$ and for the excited states, $^3P_0 \rightarrow {}^3A_{1u}$, $^3P_1 \rightarrow {}^3T_{1u}$, $^3P_2 \rightarrow {}^3E_u + {}^3T_{2u}$ and $^1P_1 \rightarrow {}^1T_{1u}$.

The $^1A_{1g} \rightarrow {}^1T_{3u}$ transition is both dipole and spin allowed. However, the $^1A_{1g} \rightarrow {}^3A_{1u}$ transition is forbidden. The $^2A_{1g} \rightarrow {}^3T_{1u}$ transition is partially allowed by singlet–triplet spin–orbit mixing. Finally, the $^1A_{1g} \rightarrow ({}^3E_u + {}^3T_{2u})$ transition is allowed due to vibronic mixing of the ^3E_u and $^3T_{2u}$ with $^3T_{1u}$.

Thus at low temperatures (*ca.* 12–80 K), we would expect absorption bands to arise from $^1S_0 \rightarrow {}^3P_1$, $^1S_0 \rightarrow {}^3P_2$ and $^1P_0 \rightarrow {}^1P_3$ transitions (in ascending energy).

At room temperature, only the $^1S_0 \rightarrow {}^3P_1$ transition occurs owing to thermal broadening and this band is commonly two or three times broader than the 12 K emission band. For Bi^{3+} the singlet–triplet spin–orbit mixing would be even stronger than for Tl^+, so a more intense band is expected.

A number of studies of the luminescence properties of Bi^{3+} activated phosphors have been reported.[1,9,40,41] For a number of Bi^{3+} activated oxides and oxychlorides, large shifts in the wavelength of emission from one lattice to another have been found.[40] It therefore appears that it is possible to explain the spectra using both localised states or a band model. The only way to really choose between the two would be by investigation of the halfwidth of the emission band. It is found that the bandwidth increases as Bi^{3+} is added to the $YNbO_4$ lattice as is apparent in Fig. 1, and assuming it is nearly symmetrical, it is much wider than found for Bi^{3+}-doped phosphors in Table 1.

The position of the broad emission band of these phosphors depends strongly on the host lattice.[40] The overall conclusion of this and other works[1,9,40] is that these materials do not contain simple Bi^{3+} centres, but that the extra absorption is due to a transition involving the Bi^{3+} ion as well as the host lattice. In fact, Blasse *et al.* invoke a band model to account for the emission band in $YVO_4:Bi$,[40] $YNbO_4:Bi$[9,40] and $Y_2WO_6:Bi$[40] phosphors.

It can now be argued that $YNbO_4:Bi$ behaves as in the model suggested in this work. Initially, at values of x around 0.0001, it can be explained by a localised state model, but as x increases, a band model takes over. Hence, overall, the explanation that initially the Bi^{3+} forms localised states above the top of the $2p(O^{2-})$ valence band, then as more Bi^{3+} ions are added, more states are introduced forming a continuous band, is reasonable.

The model of the electronic band structure for the $GdNbO_4$ system would be similar to that of Fig. 8, but the conduction band would be made up of $5d(Gd^{3+})$ orbitals and $4d(Nb^{5+})$ orbitals. However, owing to the fact that the 5d and 4d orbitals are likely to be of different energies, it is unlikely that these will overlap well and this may split the conduction band. In β-$BiNbO_4$, the Bi atoms are in very distorted square antiprismatic coordinations.[35] The initial efficiency of $GdNbO_4$ is very much weaker than that of $YNbO_4$. The reason for this, and the poorer efficiency of the $Gd_{1-x}Bi_xNbO_4$ ($x = 0.005$) may well be due to the fact that the conduction band is, in fact, narrower than in $YNbO_4$, owing to the splitting discussed above. Evidence for a narrower conduction band and some difference in the structure (possible splitting) can be observed in the diffuse reflectance spectra of $YNbO_4$ and $YNbO_4:Bi$ (Fig. 1, ref. 29) and in the fact that the emission band for $GdNbO_4:Bi$ is narrower than that of $YNbO_4:Bi$ (Fig. 1). When $x = 1.00$, *i.e.* in α-$BiNbO_4$, the orthorhombic structure contains Bi^{3+} $6s^2$ electrons located in a lone pair (which presumably has some 'p' electron character) which distorts the environment around the atom.[31]

The fact that both the pure α- and β-forms of $BiNbO_4$ contain Bi in very distorted coordinations, indicating that the $6s^2$ electrons are localised on the Bi^{3+},[10,18,22,31,50–52] means that, in this case, much of the $6s^2$ electrons lies below the O^{2-} 2p levels in Fig. 8. These pure $BiNbO_4$ materials only luminesce at low temperatures and have emission bands at 485 nm (β-phase) or 570 nm (α-phase).[9] (In the α-phase the Bi^{3+} ions have a more symmetrical coordination than in the β-phase.[9]) It is to be noted that for $Y_{0.9}Bi_{0.1}NbO_4$, the emission band is at 460 nm, thus expansion allowing distortion of the lattice causes large changes in the band structure. Not only does the band maximum no longer move so far with %Bi (as it did for $x = 0.005$ to 0.01), but also the quenching temperature is very much lower (30 K for α-$BiNbO_4$).[9]

The differences in the structures of $YNbO_4$ and $GdNbO_4$ are also implicated in the finding that when Bi^{3+} activators are present, the former lattice shows better luminance (Figs. 2

Table 1 Halfwidths of Bi^{3+} doped phosphors

	Wavelength/nm	Halfwidth/nm	Ref.
$YPO_4:Sb^{3+}$	395	143	42
$(CaZn)_3(PO_4)_2:Te$	310	41	43
$SrP_2O_7:Sn^{2+}$	464	104	44, 45
$SrB_6O_{10}:Sn$	420	68	46
$BaSi_2O_5:Pb$	350	39	47, 48
$SrAl_{12}O_{19}:Pb$	405	80	49

and 3). As Y^{3+} is smaller than Gd^{3+}, the latter distorts the Fergusonite lattice more than the former, hence the Nb^{5+} ions are in more distorted octahedral environments in the $GdNbO_4$ lattice. This extra distortion must have an effect on the band structure of the lattice, cutting down both the overlap of the O^{2-} 2p orbitals in the valence band and also of the 5d orbitals of the Gd^{3+} ions with the 4d orbitals of the Nb^{5+} ions. This may limit the mobility of the Bi^{3+} $6s^2$ non-bonding valence electrons in the $GdNbO_4$ lattice when compared to the $YNbO_4$ lattice. This limitation is in addition to that (mentioned above) caused by the splitting of the conduction band owing to the difference in energy of the Gd^{3+} 5d orbitals and the Nb^{5+} 4d orbitals.

Such limitations on the mobility of electrons in the conduction band may be manifested in the decay times of excited states. If the mobility is limited, the decay time may be shorter. It has been demonstrated that the decay time of the blue luminescence in $YNbO_4$ does indeed become shorter if Gd^{3+} is in the lattice.[23]

Conclusions

We have shown that:

1 for our new method and heating/firing regime to prepare the $Y_{1-x}Bi_xNbO_4$ lattice, a 1:1 Y to Nb ratio is optimum, whereas we previously found that use of an excess of Nb_2O_5 was necessary.

2 The composition with $x=0.005$ Bi showed higher luminance and efficiency than commercially available P47 phosphor. The Bi^{3+} activated yttrium niobate shows a blue emission at 440 nm and an efficiency of *ca.* 1.3 lm W^{-1}.

3 A simple band structure model is able to explain the movement of the emission band with an increase in concentration of the Bi^{3+} activator.

4 In symmetrical coordination, the ns^2 ions are available for delocalisation throughout the valence band. They therefore influence the luminescence properties of transition metal oxide compounds substantially. When the ns^2 ions are in more distorted environments, their influence diminishes.

Acknowledgements

We thank the EPSRC GR/L41370 for funding to carry out this work and we also thank Dr David Morton from the Army Research Lab. Washington and Dr Henry Gray from the Naval Research Lab. Washington for useful discussions. Thanks are also due to Mr David Smith for his helpful contributions. Also we gratefully acknowledge a conversation with Dr J. Robertson of Cambridge University.

References

1 G. Blasse, *Prog. Solid State Chem.*, 1988, **18**, 79.
2 G. Blasse, *J. Solid State Chem.*, 1988, **72**, 72.
3 D. M. Krol, G. Blasse and R. C. Powell, *J. Chem. Phys.*, 1980, **73**, 163.
4 M. H. J. Emond, M. Wiegel, G. Blasse and R. Geigelson, *Mater. Res. Bull.*, 1993, **28**, 1025.
5 M. Wiegel, M. H. J. Emond, E. R. Stobbe and B. Blasse, *J. Phys. Chem. Solids*, 1993, **55**, 773.
6 G. Blasse and L. G. J. de Haart, *Mater. Chem. Phys.*, 1986, **14**, 481.
7 M. Weigel, M. Hamoumi and G. Blasse, *Mater. Chem. Phys.*, 1994, **36**, 289.
8 L. G. J. de Haart and G. Blasse, *J. Solid State Chem.*, 1986, **61**, 135.
9 M. Wiegel, W. Middel and G. Blasse, *J. Mater. Chem.*, 1995, **5**, 981.
10 J. D. Donaldson and J. Silver, *Inorg. Nucl. Chem. Lett.*, 1974, **10**, 537.
11 J. Barrett, S. R. A. Bird, J. D. Donaldson and J. Silver, *J. Chem. Soc. A*, 1971, 3105.
12 D. Donaldson, D. R. Laughlin, S. D. Ross and J. Silver, *J. Chem. Soc. A*, 1973, 1985.
13 D. S. Urch, *J. Chem. Soc.*, 1964, 5775.
14 T. C. Gibb, R. Greatrex, N. N. Greenwood and A. C. Sarma, *J. Chem. Soc. A*, 1970, 212.
15 L. Atkinson and P. Day, *J. Chem. Soc. A*, 1969, 2423.
16 L. E. Orgel, *J. Chem. Soc.*, 1959, 3815.
17 S. R. A. Bird, J. D. Donaldson and J. Silver, *J. Chem. Soc. A*, 1972, 1950.
18 R. H. Andrews, S. J. Clark, J. D. Donaldson, J. C. Dewan and J. Silver, *J. Chem. Soc., Dalton Trans.*, 1983, 767.
19 J. D. Donaldson and J. Silver, *J. Chem. Soc., Dalton Trans.*, 1973, 666.
20 J. D. Donaldson, J. Silver, S. Hadjiminolis and S. D. Ross, *J. Chem. Soc., Dalton Trans.*, 1975, 1500.
21 (*a*) J. D. Donaldson, S. D. Ross, J. Silver and P. J. Watkins, *J. Chem. Soc., Dalton Trans.*, 1975, 1980; (*b*) J. D. Donaldson and J. Silver, *J. Solid State Chem.*, 1976, **18**, 117; (*c*) J. Silver, C. A. Mackay and J. D. Donaldson, *J. Mater Sci.*, 1976, **11**, 836; (*d*) J. D. Donaldson, D. R. Laughlin and J. Silver, *J. Chem. Soc., Dalton Trans.*, 1977, 966.
22 J. Barrett, J. D. Donaldson, J. Silver and N. P. Y. Siew, *J. Chem. Soc., Dalton Trans.*, 1977, 907.
23 G. Blasse and A. Bril, *J. Lumin.*, 1970, **3**, 109.
24 W. L. Wanmaker, A. Bril, J. W. Ter Vrugt and J. Broos, *Phil. Res. Rep.*, 1966, **21**, 270.
25 A. H. Buth and G. Blasse, *Phys. Status Solidi*, 1981, **64**, 669.
26 R. C. Ropp and N. J. Warren, *US Pat.*, 3 758 486, 1973.
27 D. A. Grisafe, L. Kaus and C. W. Fritsch, *US Pat.*, 3 767 589, 1973.
28 D. Charlesworth, A. Vecht and D. W. Smith, *SID Int. Symp. Digest*, 1997, **28**, 588.
29 D. Grisafe and C. W. Fritsch, *J. Solid State Chem.*, 1976, **17**, 313.
30 H. Weitzel and H. Schrocke, *Z. Kristallogr.*, 1980, **69**, 152.
31 M. A. Subramanian and J. C. Calabrese, *Mater. Res. Bull.*, 1993, **28**, 523.
32 V. I. Popolitiov, A. N. Lobachev and V. E. Peskin, *Ferroelectrics*, 1981, **40**, 9.
33 E. T. Keve and A. C. Skopski, *J. Solid State Chem.*, 1973, **8**, 159.
34 J. Robertson, W. L. Warren, B. A. Turtle, D. Dimons and D. M. Smyth, *Appl. Phys. Lett.*, 1993, **63**, 1519.
35 E. T. Keve and A. C. Skapski, *J. Solid State Chem.*, 1973, **8**, 159.
36 N. F. Mott, *Proc. Phys. Soc. London, Sect. A*, 1949, **62**, 416.
37 P. P. Edwards and M. J. Sienko, *Phys. Rev. B: Condens. Matter*, 1978, **17**, 2575.
38 C. Kittel, *Introduction to Solid State Physics*, Wiley, New York, 6th edn., 1986, ch. 8.
39 E. J. Seitz, *J. Chem. Phys.*, 1938, **6**, 150.
40 G. Blasse and A. J. Bril, *J. Chem Phys.*, 1968, **48**, 217.
41 G. Boulon, *J. Phys.*, 1971, **32**, 333.
42 J. Grafmeyer, J. C. Bourcet and J. J. Junin, *J. Lumin.*, 1976, **11**, 369.
43 R. Nagy, R. W. Wollentin and C. K. Lui, *J. Electrochem. Soc.*, 1950, **97**, 29.
44 R. C. Ropp and R. W. Mooney, *J. Electrochem. Soc.*, 1960, **107**, 15.
45 P. W. Ranby, D. H. Marsh and S. T. Henderson, *Br. J. Appl. Phys. Suppl.*, 1955, **4**, 518.
46 M. Leskela, R. T. Koskentalo and G. Blasse, *J. Solid State Chem.*, 1985, **59**, 272.
47 R. H. Clapp and R. J. Ginther, *J. Opt. Soc. Am.*, 1947, **37**, 355.
48 K. H. Butler, *Trans. Electrochem. Soc.*, 1947, **91**, 265.
49 J. L. Sommerdijk, J. M. P. J. Vestegen and A. Bril, *Philips Res. Rep.*, 1974, **29**, 517.
50 F. J. Berry and J. Silver, *J. Organomet. Chem.*, 1977, **129**, 437.
51 T. Abraham, C. Juhasz, J. Silver, J. D. Donaldson and M. J. K. Thomas, *Solid State Commun.*, 1978, **27**, 1185.
52 F. J. Berry and J. Silver, *J. Organomet. Chem.*, 1980, **188**, 255.

Paper 9/05724B